ACS APPLIED MATERIALS & INTERFACES

Research Article

www.acsami.org

High-Performance Reverse Osmosis CNT/Polyamide Nanocomposite Membrane by Controlled Interfacial Interactions

Hee Joong Kim, Kwonyong Choi, Youngbin Baek, Dong-Gyun Kim, Jimin Shim, Jeyong Yoon, and Jong-Chan Lee*

School of Chemical and Biological Engineering and Institute of Chemical Process, Seoul National University, 599 Gwanak-ro, Gwanak-gu, Seoul 151-742, Republic of Korea

Supporting Information

ABSTRACT: Polyamide reverse osmosis (RO) membranes with carbon nanotubes (CNTs) are prepared by interfacial polymerization using trimesoyl chloride (TMC) solutions in *n*-hexane and aqueous solutions of *m*-phenylenediamine (MPD) containing functionalized CNTs. The functionalized CNTs are prepared by the reactions of pristine CNTs with acid mixture (sulfuric acid and nitric acid of 3:1 volume ratio) by varying amounts of acid, reaction temperature, and reaction time. CNTs prepared by an optimized reaction condition are found to be well-dispersed in the polyamide layer, which is confirmed from atomic force microscopy, scanning electron microscopy, and Raman spectroscopy studies. The polyamide RO membranes containing well-dispersed CNTs exhibit larger water flux values than polyamide membrane prepared without any CNTs, although the salt rejection values of these membranes are close. Furthermore, the durability and chemical resistance against NaCl solutions of the membranes containing CNTs are found to be improved compared with those of the membrane without CNTs. The high membrane performance (high water flux and salt rejection) and the improved stability of the polyamide membranes containing CNTs are ascribed to the hydrophobic nanochannels of CNTs and well-dispersed states in the polyamide layers formed through the interactions between CNTs and polyamide in the active layers.

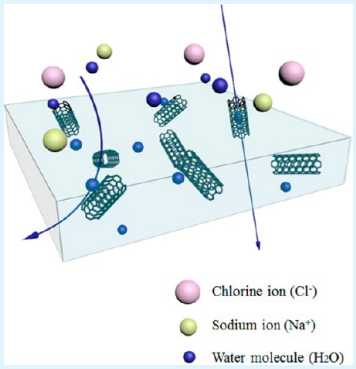

KEYWORDS: *high water flux, membranes, carbon nanotubes, interfacial interactions, water purification*

INTRODUCTION

Purification of seawater or wastewater to produce fresh water is known to be one of the most important issues in the environmental engineering and science fields, because of the current water shortage problems, mainly caused by the rapid growth of the world population and environment pollution.[1−6] A various membrane processes using different types of membranes, such as microfiltration (MF), ultrafiltration (UF), nanofiltration (NF), and reverse osmosis (RO) membranes, have been most widely used for the water purification, although other methods, such as distillation and chemical treatment, also have been used.[3,7−10] The advantages of the membrane processes are low operating temperature, low energy consumption, and high productivity.[3] In particular, the RO membrane system has been known to be most efficient to remove small-sized ions such as sodium and chloride ions in the seawater. Currently, polyamide membranes are widely used in the commercial RO systems because they offer a combination of high water flux and high rejections of the ions.[3] However, the polyamide membranes used in the RO systems has several disadvantages in the applications for desalination process, such as low chlorine resistance and low antifouling, which shortens membrane lifetime and decreases the membrane performance such as water flux and salt rejection.[3,5,6,11]

There have been many attempts to improve RO membrane performances and properties such as water permeability, salt rejection, antifouling property, and chemical/mechanical stability.[11−16] Recently, nanocomposite membranes containing nanomaterials such as metal oxide, silica nanoparticle, zeolite, graphene, graphene oxide, and carbon nanotube (CNT) have been prepared to improve these membrane properties and/or performances.[17−26] For example, titanium dioxide and silver nanoparticles were incorporated into the membranes to increase antifouling and antibiofouling properties,[19,27] and zeolite was embedded into RO membranes to improve the water flux.[18,23] In particular, CNTs have been studied for water treatment process because of its unique properties. Membranes containing CNTs have been known to have high gas or liquid permeability,[25,26,28−33] antibacterial property,[34−36] and mechanical stability.[37−40] Above all, polymeric membranes having aligned CNT structures showed ultrahigh water flux values larger than 1000 L m^{-2} h^{-1} bar^{-1} (LMH bar^{-1}).[25,26,28,30,41,42] These high water flux values of the polymeric membranes having aligned CNTs were ascribed to the unique hydrophobic character of the CNT surfaces and uniformly aligned nanosized pores of CNT materials. However, there has been no report for the preparation of polymeric membranes with aligned CNTs having large enough effective membrane area and high enough

Received: November 26, 2013
Accepted: January 18, 2014
Published: January 18, 2014

   dx.doi.org/10.1021/am405398f | ACS Appl. Mater. Interfaces 2014, 6, 2819−2829

Table 1. CNTs Having Different Amounts of Functional Groups at Different Experimental Conditions and their XPS Elemental Composition and O/C Ratio

CNT type	CNT (g)	temperature (°C)	time (h)	acid solution (mL)	C contents (%)	O contents (%)	O/C ratio
CNT1[a]					90.00	10.00	0.11
CNT2	0.2	25	3.0	20	83.42	16.58	0.20
CNT3	0.2	45	3.5	40	81.82	18.18	0.22
CNT4	0.2	65	4.0	60	78.87	21.13	0.27
CNT5	0.2	85	4.5	80	76.52	23.48	0.31
CNT6	0.2	105	5.0	100	70.68	29.32	0.41

[a]CNT1 is pristine and used as received.

NaCl rejection for practical RO membrane application, possibly because of the difficulties of incorporating uniformly aligned CNT layers into the physically stable polymer matrix materials as well as other possible technical problems.

Although the polymeric membranes with aligned CNTs for practical water treatment process have not been reported, polymeric membranes having dispersed CNTs as fillers in the polymer matrixes have been reported quite many times because the techniques to incorporate CNTs into the polymers are very well-known.[36,43,48,78−82] Therefore a various polymeric membranes containing dispersed CNTs in the selective and/or support layers were prepared and their membrane performances were measured. However when these membranes containing dispersed CNTs were used for the NaCl separation systems, most of them showed quite small salt rejection values as listed in the Supporting Information (Table S1). We believe that the small NaCl rejection values obtained from these nanocomposite membranes containing CNTs should be caused by the poor dispersion of the CNTs in the polymer matrix that generates defects, which can increase the water flux while results in decreasing the NaCl rejection efficiency. Quite large NaCl rejection values up to 98.6% were reported from the RO membranes containing zwitterion-functionalized CNTs, while their water flux values were found to be quite small about 1.33 LMH bar^{-1}, then the practical application in the RO system is not possible.[43] This small water flux value from the membrane containing the zwitterion-functionalized CNTs should be caused by the very thick polyamide layers. They probably fabricated thick polymer layers to cover the defects between CNTs and polymer matrixes, which in-turn results in the small water flux values. To the best of our knowledge, nanocomposite membrane with dispersed CNT showing high water flux in company with high salt rejection has not been reported yet.

Polymer nanocomposites have been widely used in battery researches, sensor studies, electronic devices fabrications, and other various research as well as membrane applications.[44−48] The interactions between the polymers and the nano materials have been known to be very crucial factor to impart the desired properties to polymer nanocomposite systems. Thus, various experimental methods to increase their interactions have been developed and various methods for the measurement of the interactive forces have been suggested.[36,40,49−51] It has been known that the functionality of nano materials and/or the amount of functional groups are the key parameters to increase the physical properties and/or performances of nanocomposite materials. In this work, we prepared a series of CNTs having different degree of functionality and length by changing the chemical treatment conditions. When a series of RO membranes were prepared through interfacial polymerizations of trimesoyl chloride (TMC) and *m*-phenylenediamine (MPD) with these functionalized CNTs, the degree of dispersion of the CNTs in the membranes and the interactions of the CNTs with the polymer matrix were found to affect the membrane performances. When the polyamide RO membranes were prepared with the optimized CNTs showing well-dispersed CNTs in the polymer active layers and maximum interactions between the CNTs and polymer matrixes, their salt rejection values were comparable to those of common polyamide RO membranes without any CNTs, and their water flux and membrane stability were found to be much better than those of common polyamide RO membranes without any CNTs.

EXPERIMENTAL SECTION

Chemicals and Materials. Multiwalled carbon nanotubes from Nanocyl (Belgium) were used as carbon nanotube (CNT) materials; the average diameter and average length of CNT are 10−20 nm and 10−20 μm, respectively. Polysulfone (PSf) membranes were supplied from Woong-jin chemicals (Republic of Korea) and used as a support membrane. Sulfuric acid (H_2SO_4, 98%), nitric acid (HNO_3, 60%), and isopropyl alcohol (IPA) were received from Daejung chemicals (Republic of Korea) and used as received. *m*-Phenylenediamine (MPD, 99%), trimesoyl chloride (TMC, 98%) and sodium chloride (NaCl, 99%) were supplied from Aldrich and used without any purification. Deionized (DI) water was obtained from water purification system (Synergy, Millipore, USA), having a resistivity of 18.3 mΩ cm. *n*-Hexane (95%) was received from Samchun Chemicals (Republic of Korea).

Modification of CNTs. The CNTs from Nanocyl were treated using an acid mixture (sulfuric acid and nitric acid of 3:1 volume ratio) to impart possible functional groups such as carboxylic acid by varying amount of acid mixture, reaction temperature, and reaction time. The modified CNTs were named as CNT1 to CNT6 and the number increases with the increase of the acid content in the reaction mixture and the increase of the reaction time and temperature. The experimental conditions for the preparation of the modified CNTs and their composition observed by XPS are shown in Table 1. The following procedure was used for the preparation of CNT4 and it was applied to prepare the composite RO membranes showing best membrane performance. Two-tenths of a gram of pristine CNTs and 60 mL of acid mixture solution were placed into a 100 or 250 mL round-bottom flask equipped with a magnetic stirring bar and the mixture was sonicated for 30 min. The flask was then placed into an oil bath thermo stated at 65 °C with stirring. After 4 h of reaction, the solution was cooled to room temperature and diluted with 1.5 L of water. The diluted solution was filtered by anodic aluminum oxide (AAO) filter whose pore size is 0.2 μm. Water was poured onto the filtering system until a neutral pH is attained. The resulting CNTs on filter were dried in the 35 °C vacuum oven.

Preparation of the Polyamide Membranes with CNT and without CNT (PA-CNT and PA Membrane). Polysulfone support membrane was treated with IPA for 10 min to enlarge pores and washed several times with water. The pretreated membrane was placed in the water bath for 3 h to stabilize the pores. A series of aqueous solution were prepared with 2 wt % MPD and 0.002 wt % various types of CNTs prepared using different reaction conditions. Another series of aqueous solutions were prepared with different amounts of

CNT4 and MPD. Fifteen-hundredths of a gram of TMC was added into a 250 mL round-bottom flask equipped with a magnetic stirring bar in glovebox filled with argon gas. *n*-Hexane (149.85 g) was added into the flask using a syringe, and the solution was stirred at room temperature. Polysulfone membrane was placed into the bath with 500 g of aqueous solution. After 3 h, membrane was taken out and air bubbles and droplet of aqueous solution formed on the membrane surface were removed by rolling a rubber roller. The membrane was fixed on the acryl flat board with rubber mold. The TMC solution was poured on the membrane saturated with the aqueous solution. After 60 s, the excess of organic solution on the membrane was removed and the membrane was placed in the 100 °C oven for 5 min to induce cross-linking as well as further polymerization. The resulting membrane was then washed with water several times. The prepared composite membranes with and without CNTs were named as PA-CNT membrane and PA membrane, respectively.

Membrane Filtration Test. Water flux and salt rejection values were obtained by two test method such as dead-end filtration cells (CF042, Sterlitech Corp., Kent, WA) and lab-scale cross-flow RO membrane test unit. The effective membrane areas were $2.16 \times 2.16 \times \pi$ cm^2 and 3.3×6.8 cm^2 with the 0.3 cm of channel height, respectively. The pressure was maintained at about 15.5 bar (225 psi) and the feed solution was 2,000 mg L^{-1} of NaCl solution whose conductivity was about 3.86 mS cm^{-1}. These membrane operating conditions have been generally used in the BWRO membrane researches by others.[5,23,73,78] Cross flow velocity at the membrane surface was 700 mL min^{-1} in cross-flow system. Water flux was measured by weighing the permeate solution after the membranes were compressed for 1 h at 15.5 bar. Membrane flux, J, was calculated using eq 1

$$J = \Delta V/(A\Delta t) \quad (1)$$

where ΔV is the volume of permeate collected between two weight measurements, A is the membrane surface area, and Δt is the time between two weight measurements.

Salt rejection was calculated using the following eq 2

$$R = (1 - C_p/C_f)100\% \quad (2)$$

where R is salt rejection parameter, C_p is the salt concentration in permeate, and C_f is the salt concentration in feed. The salt concentrations were measured using conductivity meter (InoLab Cond 730P, WTW 82362, weilheim). All membrane performance results shown in the Figure 1 and Table S2 in the Supporting Information are the average values obtained by more than three measurements from the three membrane samples prepared at different times.

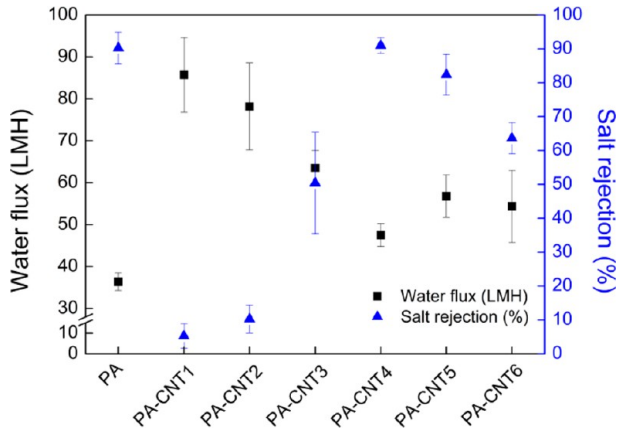

Figure 1. Water flux and salt rejection of membranes prepared by various types of CNT (tested by dead-end filtration, 2000 ppm of NaCl feed solution, 15.5 bar of feed pressure).

Interaction Force Measurement. The interactive forces between the CNT and polyamides were measured by an atomic force microscope (AFM, Seiko Instrument, SPA-400, Japan).[52] AFM tip could not be coated with the polymers by the coating method because cross-linked polymers are obtained from the polymerization of MPD and TMC and the resulting polymer, polyamide, is insoluble in any common solvents such as tetrahydrofuran (THF), dimethylromamide (DMF), dimethyl sulfoxide (DMSO), and dimethylacetamide (DMAc). Therefore the polyamide unit could be tethered on the AFM tip from the following procedure (see Figure S1 in the Supporting Information). A silicon cantilever (Nanosensors, CONTR) was washed with IPA, ethanol and water subsequently dried with N_2 gas. Then the tip was treated with oxygen plasma (150 W, 30 s) and it was chemically modified with 3-aminopropyltriethoxysilane toluene solution (10 mM) for 2 h at room temperature. This amine terminated AFM tip was further treated with TMC (0.1 wt % in *n*-hexane) for 30 min, which was followed by reaction with MPD in water (2 wt %) for 30 min. Then, the tip was washed with ethanol and dried in the natural air. The silicon wafer was modified from the same procedure used for the modification of the AFM tip to confirm the modification of the tip because the size of the tip is too small to be analyzed. Surface composition analysis of modified silicon wafer and PA membrane is shown in Table S3 of the Supporting Information. CNT films were prepared by filtering procedure as reported by others.[53] Five milligrams of CNT (pristine and functionalized) was dispersed in 200 mL of water using sonication bath and the CNT dispersed solution was filtered by AAO filter. Then the flat CNT film on the filter was obtained and dried in the air.

As pristine or functionalized CNT film approached the polyamide (PA)-modified AFM tip, an interaction was generated between the surface of CNT film and the tip, inducing a cantilever deflection. The interaction force could be calculated by multiplying the spring constant of the cantilever by the deflection distance. The force could be detected in the same manner as the CNT film was retracted. Then, the force−extension curve could be constructed from these measurements. We used a spring constant of 0.2 N m^{-1}, supplied by the manufacturer. A speed of 0.2 μm s^{-1} was applied to obtain the force extension curves during approach and retraction of the surface of CNT film from the PA-modified tip. All experiments were carried out in the air at room temperature. Approximately 100 approach/retract cycles were carried out for each CNT sample.

Raman Spectroscopic Mapping. Raman spectroscope (LabRam ARAMIS, Horiba Jobin-Yvon, France) was used for the Raman spectroscopic mapping of PA membrane, PA-CNT membranes, polyamide, and CNT. Thin active layers of PA and PA-CNT membranes were transferred on the silicon wafer because fluorescences from polysulfone could disturb detecting the Raman scattering from polyamide and CNT. Nonwoven felt layer was taken off with sharp tweezers from thin film composite membrane. Then, polyamide layer on polysulfone membrane was placed on the silicon wafer. Purified THF was dropped slowly on the membrane until all of polysulfone layer was dissolved, and then the remaining polyamide layer was removed from the silicon wafer. Very thin polyamide layer was obtained after drying in vacuum oven at 30 °C for 24 h. The excitation source was a diode laser with an excitation wavelength of 785 nm and a power of 5 mW. The laser excitation was focused using a 100× objective and the Stroke-shifted Raman scattering was recorded using a 1400/600 groove min^{-1} grafting. Raman mapping images were collected within a 15×15 μm^2 area of the active layer of the membrane on a silicon substrate in order to visualize the distribution and interaction of the CNT in the polyamide matrix. The Raman mapping images of the membranes were obtained by integrating the area of maximum peak intensity ($\pm$10 cm^{-1}).

Characterizations. Morphology of CNTs prepared with different reaction conditions was observed by transmission electron microscopy (TEM, LIBRA 120, Carl Zeiss, Germany). One milligram of CNT was dispersed in 50 mL of water using sonication bath and then the dispersed solution was dropped on the carbon grid. The grid was dried in the 35 °C vacuum oven over 8 h. For the observation of membrane cross-sectional images by TEM, small pieces of the membrane samples

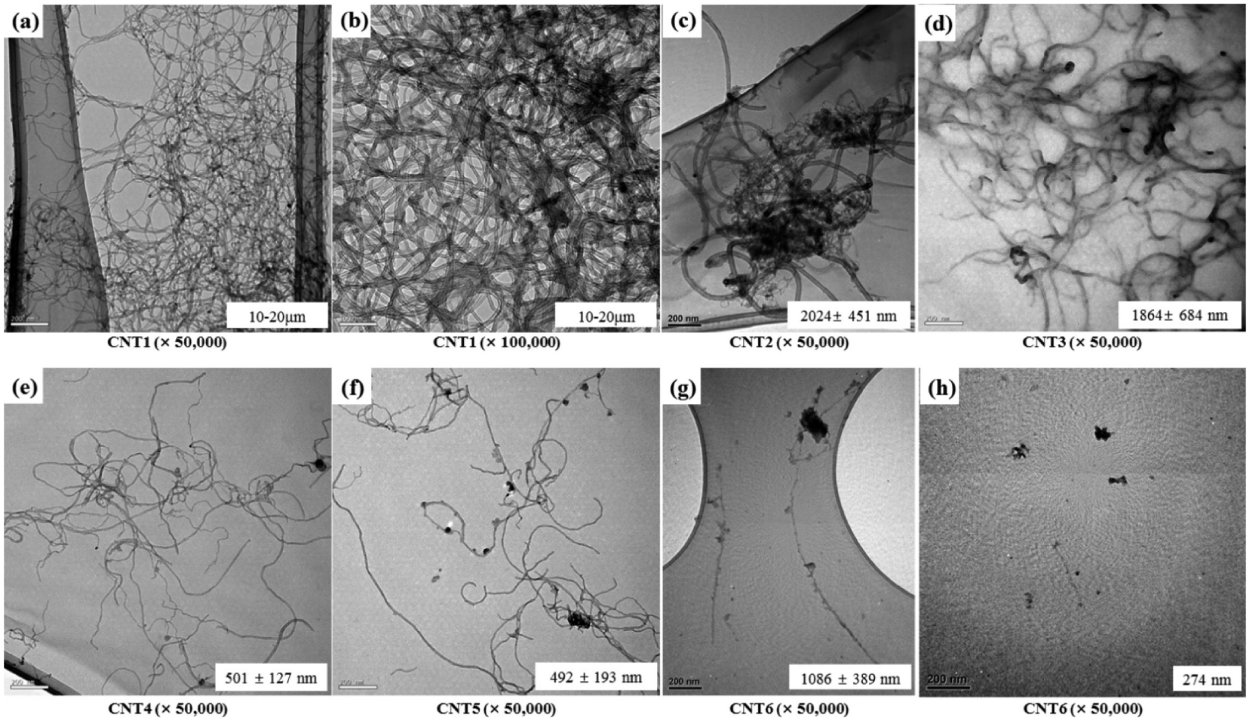

Figure 2. TEM images of each CNT treated using the acid mixture at different reaction conditions: (a, b) CNT1, (c) CNT2, (d) CNT3, (e) CNT4, (f) CNT5, and (h, g) CNT6 (scale bar = 200 nm).

were embedded in Spur resin. Approximately 60−70 nm thick sections were cut by an ultramicrotome (MTX, RMC) and placed on TEM grids. The sections were observed at an accelerating voltage of 120 kV. The surface compositions of the CNTs, membranes, and silicon wafer modified by the polyamide unit were analyzed by X-ray photoelectron microscopy (XPS, PHI-1600) using Mg Kα (1254.0 eV) as radiation source. Survey spectra were collected over a range of 0−1100 eV, followed by high resolution scan of the C 1s, O 1s, and N 1s regions. Surface morphologies of the membranes were inspected by scanning electron microscopy (SEM, JSM-6701F, JEOL) using a field emission scanning electron microscope (FESEM).

RESULTS AND DISCUSSION

Modification of CNTs. The pristine CNTs were treated using the strong acid mixture of sulfuric acid and nitric acid in 3:1 volume ratios by varying the amount of acid mixture, reaction temperature, and reaction time (Table 1) to prepare CNTs having acid functional groups.

Although there are only 5 different acid-treated CNTs in Table 1 used in this study, we prepared more than 35 different CNTs having different degree of functionality as shown in the Supporting Information (Figure S3). Since our main objective in this study is to observe the effect of the functionality of CNT on the interaction with polyamide and to prepare the membrane with high salt rejection value by controlling the interfacial interactions between CNT and polyamide matrix, 5 different CNTs having various O/C ratio values were chosen to observe the interfacial effects on membrane performances.

We could conclude that the acid groups such as carboxylic acid are attached on the CNT surface during the modification process from our XPS, TEM, Raman spectroscopy results. Others also reported the incorporation of carboxylic acid groups on the CNT from the acid treatment.[35,54] The detailed discussions about the XPS, TEM, and Raman spectroscopy results are listed in the later part of this manuscript. We intentionally imparted the acid groups on the surface of CNTs to disperse the CNTs in the aqueous solution well, then it is possible to prepare polyamide active layer containing well-dispersed CNTs from the interfacial polymerizations. Also, it was expected that the acid functionalized CNTs could have interactions with the polyamide through the H-bonding and/or dipole−dipole interactions. The interaction was confirmed by AFM studies shown in the later part of this manuscript.

Surface compositions of the CNTs such as CNT1 to CNT6 prepared from the different conditions were characterized by XPS analysis (Table 1 and Figure S2 in the Supporting Information). The content of oxygen increases as the increase of the amount of the acid mixture, reaction temperature, and time. The atomic ratios of oxygen to carbon (O/C) indicate the contents of acid groups on the CNT surface by the acid treatment. The acid group formed on CNT can increase the dispersion of CNTs in the aqueous solution and in the polyamide matrix by the H-bonding and/or dipole−dipole interactions.

Membrane Filtration Test. Because the dead-end membrane filtration test is simpler than the cross-flow filtration, the screening test to evaluate the membrane performance of PA and PA-CNT membranes were carried out using the dead-end filtration method. While the detailed studies for the membrane tests were done using the cross-flow filtration method shown in the later part of this manuscript. Water flux and salt rejection values of PA and the PA-CNT membranes containing CNT1 to CNT6 are shown in Figure 1. These membranes were prepared using aqueous solutions with 0.002 wt % CNT and 2 wt % MPD and 0.01 wt % organic solution with TMC, respectively. All the membranes containing CNTs showed larger water flux values than PA membrane without CNT (36.4 LMH), whereas the salt rejection values of PA-CNT1, PA-CNT2, PACNT3, and PA-CNT6 membranes are smaller than that of the PA membrane. Interestingly, water flux value of PA-CNT4 membrane was found to be larger than that of PA membrane

and the salt rejection value of PA-CNT4 membrane is close to PA membrane. This remarkable membrane performance behavior was further studied by exploring the interaction behavior of the CNTs and the polyamide and the dispersion of the CNTs in the polar matrix such as the polyamide and water.

Effects of Interaction and Dispersion of CNTs on Salt Rejection. TEM, SEM, AFM, and Raman mapping analysis were performed to elucidate the changes of the salt rejection and water flux values of PA and PA-CNT membranes. Because the polyamide, the active layer, is prepared by interfacial polymerization using aqueous solution containing CNTs with organic solution, the dispersion of CNTs in the water is very important to obtain the polymers having well-dispersed CNTs. 0.002 wt % of CNT aqueous solution (0.02 mg mL^{-1}), the same concentration of CNTs in the aqueous solutions used for the interfacial polymerization, was used to obtain the TEM images (Figure 2). If CNTs are well dispersed in this solution, then it is very possible that CNTs in the polymerization solution should be well-dispersed. TEM image of CNT1, the pristine CNT without any acid treatment, shows the bundle morphology without any dispersed structures. Similar bundle or entangled structures were observed from CNT2 and CNT3 (Figure 2b–d) although they are less entangled than CNT1. For the CNT4 and CNT5, prepared from harsher conditions, such entanglements disappear and well dispersed CNT structures were observed, while it is also clear that CNTs were cut down to shorter tubes.[54,55] For CNT6, prepared by the harshest condition, does not have much tube structures, whereas mostly small spots possibly composed of debris of carbon materials were observed (Figure 2g, h). Because CNT1 to CNT3 are not fully dispersible in water, those aggregated structures can be transferred into polyamide forming aggregated domains working as defects in PA-CNT membranes, which can decrease the salt rejection values for the PA-CNT membranes prepared from these CNTs. We strongly believe that the large salt rejection values of PA-CNT membranes prepared using CNT4 and CNT5 should be related to this well-dispersed CNT morphology in water. The well-dispersed CNTs in those PA-CNT membranes can minimize the defects in the membrane, so their salt rejection values are close to or even larger than that of PA membrane. PA-CNT6 membrane shows smaller salt rejection value and slight larger water flux value. The aggregated particles, produced by the oxidation reactions of very harsh condition, possibly generate some defect structures in the polyamide layers that in turn can increase the water flux. Still the water flux value of PA-CNT6 membrane is smaller than that of PA-CNT2 and PA-CNT3 membranes because CNT6 is more functionalized than CNT2 and CNT3, then CNT6 can be more interactive with the polymers than CNT2 and CNT3. As a result, although there are defects in PA-CNT6, they are less than in those in PA-CNT2 and PA-CNT3 membranes.

Surface morphology of PA and PA-CNT membranes was observed from SEM images (Figure S4 in the Supporting Information). Similar noodle structures from polyamide were observed on the surfaces of the PA and PA-CNT membranes, similarly as previously reported.[56−59] Large clusters from aggregated CNTs were observed on the PA-CNT membranes prepared using CNT1 and CNT2 (Figure S4c–e in the Supporting Information), while small clusters were observed on the PA-CNT6 membrane. These large and small clusters were formed from aggregations of CNTs in aqueous solution. On the contrary, two bundles of CNTs were observed from the PA-CNT4 membrane, as shown in Figure S4f of the Supporting Information and such one or two bundles of CNTs were observed all over the surfaces of the PA-CNT4 membrane, indicating that CNTs are well dispersed. We tried to observe the bottom side of active layer of PA and PA-CNT4 membrane (see Figure S5 in the Supporting Information). In contrast to the clean and uniform images of the PA membrane, the bottom part images of the PA-CNT4 membrane shows several in and out lines from a single bundle of CNTs. Because the density of CNT (1.3−1.4 g cm^{-1}) is larger than that of the aqueous solution, CNTs sink into the bottom part during the membrane preparation procedures. Therefore, the bottom side image of PA-CNT membrane shows a larger amount of CNTs than the top side images. The longer or shorter line images might indicate that the CNTs are located more or less parallel or tilted to the polyamide layer. The brightness changes of the longer lines might indicate the location of CNT stems at different heights. The diameter of the CNT shown in Figure S5c in the Supporting Information, about 17 nm, is within the range of the diameter of the CNT, 10−20 nm. We also tried to observe the membrane cross-sectional images by TEM (Figure S6 in the Supporting Information). PA, PA-CNT1, and PA-CNT4 membranes exhibited nanoscale surface roughness ranging from 100 to 400 nm thickness. Because the content of CNTs in the membranes are very small (0.002 wt % CNT and 2 wt % MPD, respectively in the polymerization solution), it was quite difficult to observe the CNTs in the cross-section. However, it was very clear that PA membrane does not show any CNT images in the polyamide layer, while a few of the cross sections from the PA-CNT1 and PA-CNT4 membranes clearly show the CNTs in the polyamide layers. CNTs are mostly entangled on the membrane surface in the PA-CNT1 membrane whereas, a few bundles of CNTs with dispersed structures were observed mostly at the bottom side of the PA-CNT4 membrane as shown in the Supporting Information.

Raman spectroscopic mapping was carried out to further confirm the spatial distribution of CNTs in the polyamide membranes. Raman spectroscopic mapping has been utilized to visualize spatially the distribution of CNTs or other nanomaterials in other matrix materials including polymers.[51,60−64] Figure 3c shows the Raman spectra of polyamide, CNT1, and CNT4; distinct characteristic peaks of polyamide and D and G bands of CNT were observed at 998, 1308, and 1600 cm^{-1}, respectively. The D/G ratio, the peak intensity ratios of D band and G band, of CNT4 (1.81) is larger than that of CNT1 (0.32), indicating that the acid treatment for the functionalization increases the defects on CNT surfaces. Similar results increasing the D band intensity by the functionalization were reported by others before.[54,65] Raman mapping images were collected within a 15 × 15 μm^2 area of the PA-CNT membrane surfaces in order to visualize the dispersion of CNTs in the polyamide and the interactions of CNTs with the polyamide (Figure 3a,b). The Raman mapping of the PA-CNT membrane was obtained by integrating the area of the three peaks at 998 cm^{-1} for polyamide and at 1308 and 1600 cm^{-1} for CNTs, where the green and red regions represent polyamide and CNT, respectively. Figure 3a illustrates the Raman mapping of the PA-CNT1 membrane, in which green and red area were separated, indicating that CNT1 is aggregated in the polyamide. On the contrary well-dispersed image of red and green colors is observed from the Raman mapping of PA-CNT4 membrane, indicating that CNTs are well-dispersed in the polyamide layers. Raman spectra of regions (1), (2), and (3) in panels a

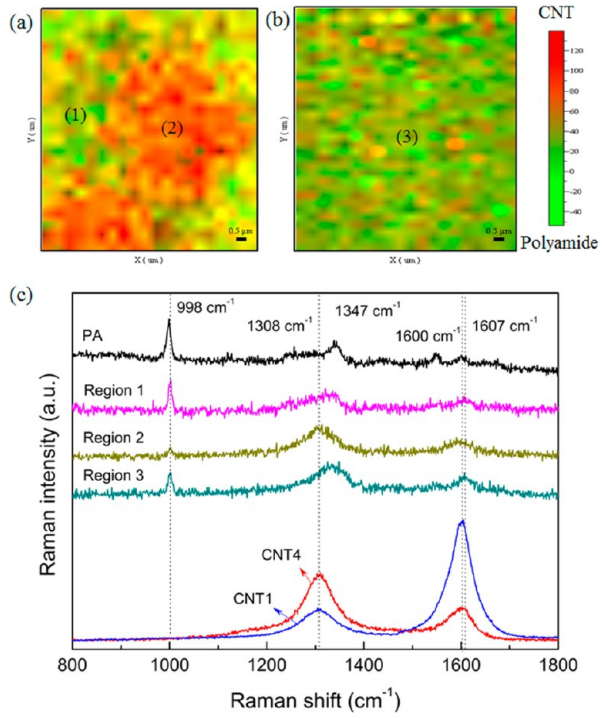

Figure 3. Raman spectroscopic mapping images of (a) PA-CNT1 and (b) PA-CNT4 membrane and (c) Raman spectra of polyamide, CNT1, CNT4, and regions (1), (2), and (3) in Raman mapping area.

and b in Figure 3 are shown in Figure 3c. The Region (1) Raman spectrum shows mostly polyamide peak and region (2) Raman spectrum shows mostly CNT peaks, and the region (3) Raman spectrum shows both CNT and polyamide peaks. Therefore, in most areas of PA-CNT4, both CNT and polyamide are well-mixed because of the interactions between the two materials. The D and G bands in the region (3) Raman spectrum of PA-CNT4 membrane shifted from those in CNT, whereas no shift was observed for the peak from polyamide. L. Bokobza et al. reported that these CNT peaks from Raman spectra shift to higher wavenumbers because of the decrease in the intertube interactions when CNTs are debundled or well-dispersed.[66] In addition, a larger shift of D band than G band is also reported when there are interactions between CNTs and matrix materials.[66−68]

For the detailed and systematical investigation of the interactive forces between polyamide and CNT1 to CNT6, AFM analysis was carried out. The interaction between CNT and polyamide should be the important parameter that determines compatibility between CNTs with polyamide and the membrane performances of the PA-CNT membranes. Because the AFM tip was modified to have the amide groups in the polyamide units and the amine groups in the MPD monomer (see Figure S1 in the Supporting Information), the interactive forces between the modified AFM tip and the CNTs recorded by AFM analysis can represents interactions between the CNTs with the amide groups and/or with amine groups. Therefore the chemical composition of AFM tip surface is similar to the compositions of the membranes and also to those in the interfacial polymerization systems. It is well-known that carboxylic acid groups (which are attached on the CNTS) can have dipole−dipole interactions and/or hydrogen bondings with amide and amine groups.[86] Similar AFM analysis has been widely used to measure the interactive forces between CNT and polymers in the composites.[52,69] Figure 4 shows the mean interaction forces of polyamide-modified tips for the flat films

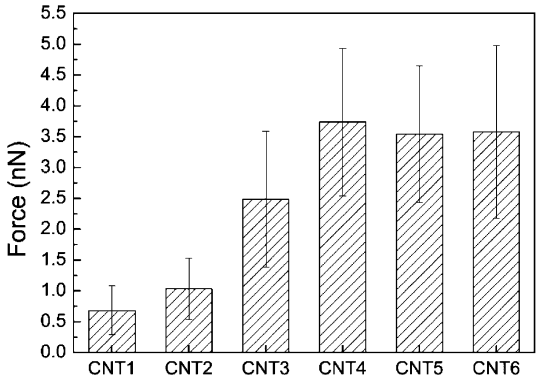

Figure 4. Mean interaction forces with standard deviations of polyamide-modified tips for the flat plates of CNT1 to CNT6.

of CNT1 to CNT6. Typical force−extension curves and interaction force histograms are also shown in the Supporting Information. Because uneven CNT powders can affect the interaction forces between CNT and polyamide-modified tip, thin and even CNT films deposited on the AAO membrane were intentionally used. Small mean interaction forces were recorded for both CNT1 (0.68 ± 0.40 nN) and CNT2 (1.03 ± 0.50 nN) films, whereas a larger pull-off force about 3.74 ± 1.20 nN, indicating the larger negative values, was observed for CNT4; this value is about 5.5 times larger than that for CNT1. The interaction force behavior of the CNT films for CNT1, CNT2, CNT3, and CNT4 was found to be same as the salt rejection behavior for PA-CNT1, CNT2, CNT3, and CNT4 membranes; the interaction force and salt rejection both increase from CNT1, CNT2, CNT3, to CNT4. Although interactive forces for CNT4, CNT5, and CNT6 with polyamide were quite close, the salt rejection value of PA-CNT6 membrane is quite smaller than those of PA-CNT4 and PA-CNT5 membrane. Since CNT6 was prepared from harshest oxidation condition, it has a large number of acid groups to have quite large interactive forces with polyamide, whereas the aggregated structure of CNT6 in the aqueous solutions used in the interfacial polymerization could be transferred into the polyamide layers and the defect structures generated from the aggregation decrease the salt rejection (Figure S4g, h in the Supporting Information). Therefore, since CNT4 and CNT5 have larger interactive forces with polyamide and aggregation-free structures, PA-CNT membranes prepared from these CNTs show larger salt rejection values than those prepared from less-functionalized CNTs (CNT1, CNT2, and CNT3) and overfunctionalized CNT6.

Membrane Performance of PA-CNT4 Membrane. Both PA-CNT4 and PA-CNT5 membranes show very good membrane performance behavior (high water flux and salt rejection) and CNT4 and CNT5 show the larger interactive forces with polyamide than other CNTs. Still, the salt rejection value of PA-CNT4 membrane is larger than that of PA-CNT5 membrane and the interactive force of CNT4 is also slightly larger than that of CNT 5, whereas the PA-CNT5 membrane shows a larger water flux value than PA-CNT4 membrane, although their differences are not great. For our convenience to derive the conclusion of this study, the detailed data on the

membrane performance of the PA-CNT membranes are focused on PA-CNT4 membrane.

We could prepare a series of PA-CNT4 membranes by changing the MPD and CNT4 concentrations in the interfacial polymerization, while we could not change the TMC concentrations because the solubility of TMC is too low (only 0.1 wt % TMC solution was used) to change. Figure 5

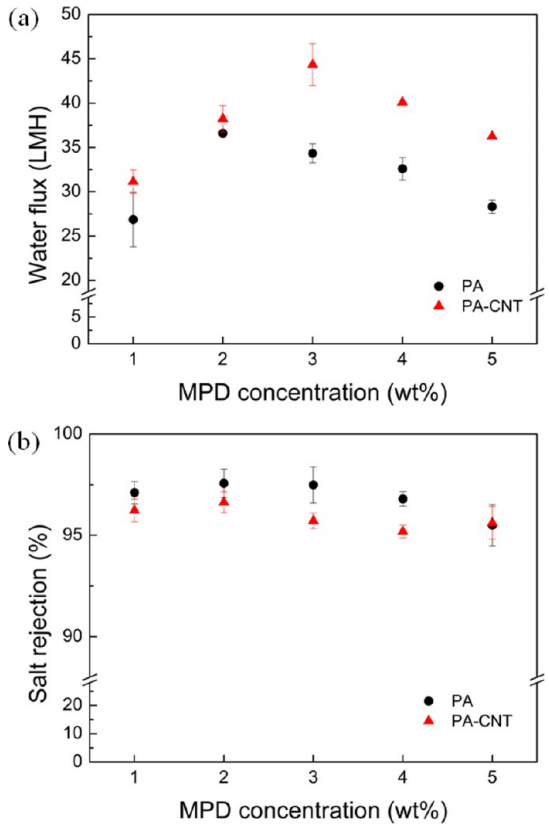

Figure 5. (a) Water flux and (b) salt rejection of PA membrane (prepared by 2 wt % of MPD in aqueous solution) and PA-CNT4 membrane (prepared by 2 wt % MPD and 0.001 wt % CNT4 in aqueous solution) (tested by cross-flow filtration, 2000 ppm of NaCl feed solution, 15.5 bar of feed pressure, 700 mL min^{-1} of cross-flow rate).

and Table S2 in the Supporting Information shows the water flux and salt rejection values of the membrane prepared by various MPD and CNT concentrations. It is well-known that salt rejection values measured by cross-flow filtration are usually larger than those measured by dead end filtration. For the comparison of the membrane performance of PA and PA-CNT membranes, the dead end filtration method was used due to the convenience of the method, while for the detailed study of the membrane performance of PA-CNT4 membranes, the cross-flow filtration method was used because it is close to the practical RO membrane filtration system. When PA-CNT4 membrane was prepared using the aqueous solution containing less than 0.0002 wt % of CNT, water flux and salt rejection values were found to be close to those of PA membrane. For example, water flux and salt rejection values of PA-CNT4 membrane prepared using aqueous solution containing 0.00004 wt % of CNT were 34.81 LMH and 97.50%, respectively. It is clear that the very small amount of CNT does not affect the membrane performances. In contrast, when PA-CNT4 membrane was prepared using the aqueous solution containing larger than 0.005 wt % of CNT, a large increase of water flux and a large decrease of salt rejection were observed. For example, very large water flux of 52.64 LMH and very small salt rejection of 18.86% were observed from PA-CNT4 membrane prepared using aqueous solution containing 0.025 wt % of CNT. This result indicates that a larger amount of CNT (larger than 0.025 wt %) decreases the membrane performance, possibly because of the formation of aggregated CNT bundles in the polyamide (see Figure S9 in the Supporting Information). Therefore, from 0.0005 to 0.005 wt % of CNT concentrations in the aqueous solution were used for the preparation of PA-CNT4 membranes.

Most of the PA-CNT4 membranes show larger water flux value than PA membrane when the same amount of MPD (the same concentration of MPD in aqueous solution) was used. It was also found that PA-membrane prepared by 2 wt % of MPD shows the largest water flux with a large enough salt rejection value (Table S2 in the Supporting Information). It is very possible that there is an optimized monomer concentration ratio for the interfacial polymerization to produce polyamide active layers having optimized cross-linking density, polarity, and polymer structure to give maximum water flux and salt rejection values. For example, if the cross-linking density of polyamide is very high (it could be obtained using large amount of trifunctional TMC in the polymerization), water flux through the polymer layer could be interrupted because densely packed polymers normally have smaller free volumes.[16] We could obtain maximum water flux value from PA-CNT4 membranes when 3 wt % of MPD in aqueous solution was used, while the maximum water flux value from the PA membrane was obtained when 2 wt % of MPD was used. Therefore slightly larger amount of MPD is needed to obtain the maximum water flux for the PA-CNT4 membranes than for the PA membrane. The functionalized CNTs having carboxylic acid groups on CNTs can form salt structure with the amine groups of MPD in aqueous solution and the hydrogen bonding between the acid groups on CNT and amine groups is also possible. Then some of the amine groups in MPD complexed with the acid groups on the CNTs cannot go through the polymerization, and a slightly larger amount of MPD (1 wt % for our case) is needed to get the polyamide structure showing maximum water flux. The maximum water flux of the PA-CNT4 membrane is larger than that of PA membrane by 7.65 LMH (17.2% increase), while slightly smaller salt rejection value by 2.24% was observed. A schematic illustration demonstrating the fast water transport of water molecules through the PA-CNT membrane is presented in Scheme 1. CNTs are well-dispersed in the polyamide membrane and this membrane structure can offer the fast transport way to pass water molecules. Water molecules can go into the inside of CNT by capillary force because of the nanosized capillary structure of CNT and they can pass through the hydrophobic inner side of CNT.[28,30,41,42] Therefore, the possible pathway of water molecules through polyamide matrix could be shorten resulting in the increase of the water flux. Hydrated ions of sodium and chlorine can also pass through the CNT channel quickly, because diameter of CNTs in the membrane is large enough to pass ions with water. According to the previous studies,[46,84,85] CNTs with diameters in the range of 0.6−1.1 nm can exclude the ions from water. Therefore, the high salt rejection values of our membranes indicates that polyamide covering well dispersed CNTs can reject the ions. Water molecules can go through the way between polyamide matrix and the wall surface of CNT, which

Scheme 1. Schematic Illustration of the Fast Transport of Water Molecules

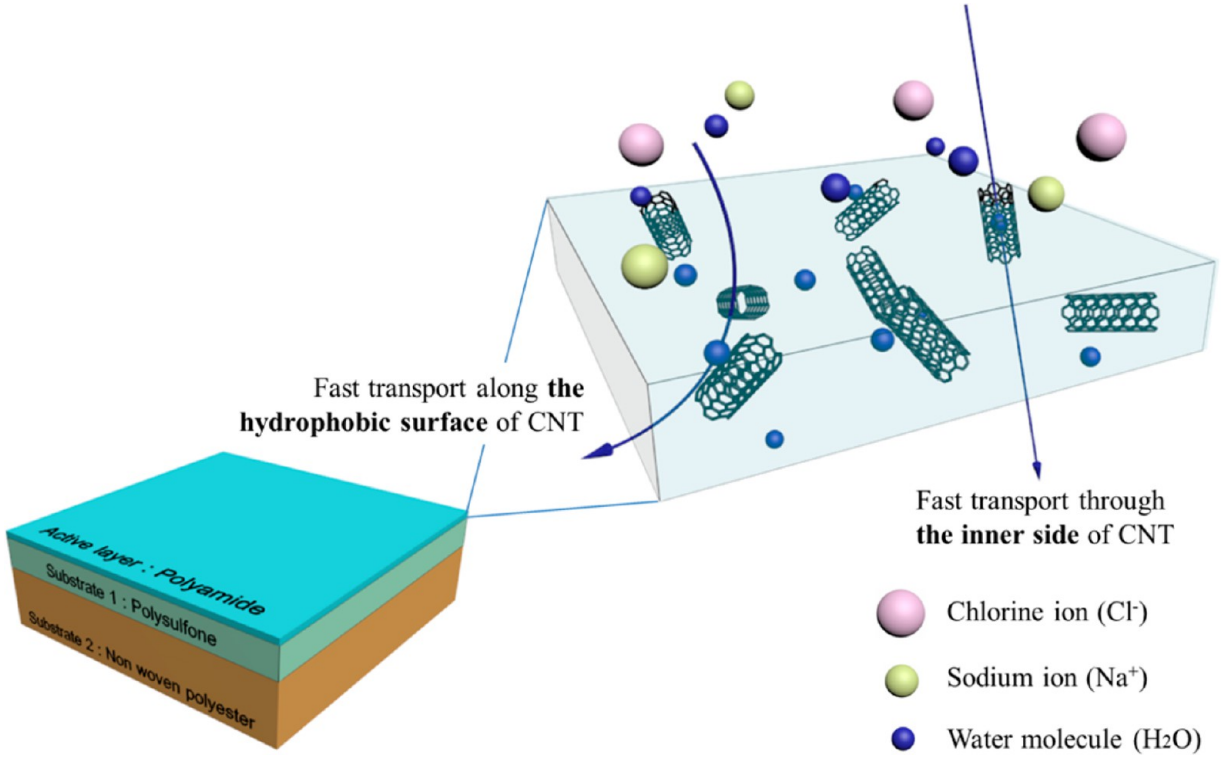

has a relatively hydrophobic nature. Although the CNT surface was functionalized by acid groups, it is still very possible that many parts of the CNT surfaces are intact, then water can slide quickly on the surface. Similarly, others reported that nanofillers like zeolite in the polymer membrane can increase the water flux because the space produced between fillers and polymer matrix can give the fast path for the water molecules.[18,23] In our case, PA-CNT4 membranes containing well-dispersed functionalized CNTs in the polymer matrix show larger water flux values with the relatively small decrease of the salt rejection values, whereas PA-CNT1 to −CNT3 membranes having coagulated CNTs show very large water flux and very small salt rejection values. Therefore, CNTs can increase the water flux because of its hydrophobic nature and high salt rejection can be observed only when CNTs and polyamide have high interactive forces to form well-dispersed CNT structures producing defect-free membrane layers.

In addition, the CNTs having acid groups can increase the hydrophilicity of the membrane which also can increase the water flux. Contact angles of the membranes were measured by the captive bubble method because it is more accurate than the sessile drop method for the RO membrane surfaces as reported in our previous work.[83] As shown in Figure S10 in the the Supporting Information, the air contact angle value of PA-CNT1 membrane is slightly larger than that of PA membrane possibly because the small amount of hydrophobic pristine CNTs can increase the hydrophobicity on the surfaces. While, the air contact angle of PA-CNT4 membrane was found to be smaller than those of PA and PA-CNT1 membranes because hydrophilic CNT4 is incorporated into the membrane. Although the contents of CNTs in the membrane is very small, the water droplet having diameter in range in the range 2−4 mm can be contacted with some of the CNTs, which can affect the changes of the contact angle.

Durability of PA-CNT4 Membrane. Water flux and salt rejection values of PA and PA-CNT4 membranes were measured with time using pure water and NaCl feed solution (Figure 6). The water flux of PA membrane decreased by 32.80% after 48 h, whereas that of the PA-CNT membrane decreases by only 18.40%. The decrease of the water flux in pressure driven system has been known to be caused by the compression of the membranes.[36,55] This behavior could be further proved by the operation at high pressure, such as 40 bar of feed pressure. In addition, we also performed the membrane performance test using the commercialized membrane (LFC-1 membrane) for BWRO membrane received from Hydranautics. Flux decrease of PA-CNT4, LFC-1, and PA membranes under the 40 bar of feed pressure were 18.11, 22.10, and 42.15%, respectively (see Figure S11 in the Supporting Information). Possibly, one of the most important advantages of CNTs using as filler in the nanocomposite materials is the increase of physical properties including the mechanical stability. Nanofillers including CNTs in the polymer matrix can disturb the polymer chain mobility to form the compressed polymer packing structures.[56] Therefore the polyamide layer in PA-CNT4 membrane can be less compressed than that in PA membrane and which in turn results in the less decrease of water flux in the PA-CNT4 membrane than that in the PA membrane. There are a number of reports that even a small amount of CNT (less than 0.5 wt %) can increase the mechanical property of the nanocomposites.[40,57] In addition, the larger tensile strength and Young's modulus of PA-CNT4 than those of PA could be strongly related to the durability of PA-CNT 4 membrane at high pressure (Figure S12 in the Supporting Information).

Similarly, a smaller decrease in water flux on PA-CNT4 membrane were observed when 2000 ppm NaCl solution was used for feed solution from 0 to 10 h of cross-flow filtration

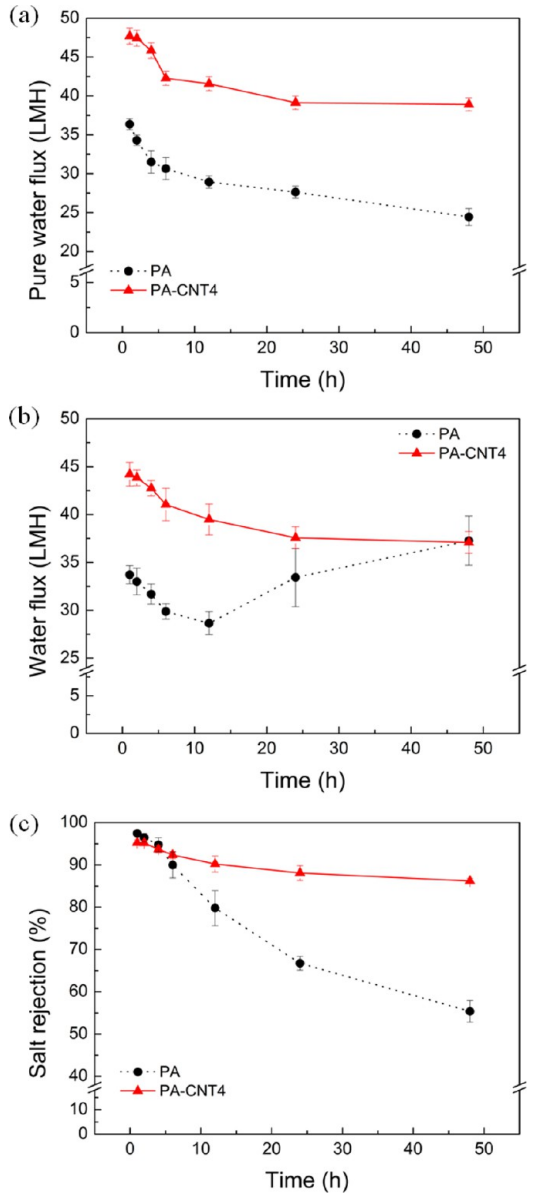

Figure 6. Water flux and salt rejection measurement with time: (a) pure water flux, (b) water flux, and (c) salt rejection of 2000 ppm NaCl solution of PA membrane (prepared by 2 wt % of MPD) and PA-CNT4 membrane (prepared by 3 wt % of MPD and 0.001 wt % of CNT4) (tested by cross-flow filtration, 2000 ppm of NaCl feed solution, 15.5 bar of feed pressure, 700 mL min^{-1} of cross-flow rate).

experiment. After 10 h, the water flux of PA-CNT4 membrane decreases continuously, while that of PA membrane starts to increase as shown in Figure 6b. The increase of the water flux of PA membrane could be correlated with the large decrease of the salt rejection after 10 h. It is well-known that the polyamide layers without any filler can be damaged by chlorine.[12,14,58,59] Therefore, the large decrease of the salt rejection and the large increase of the water flux after 10 h of operation should be caused by the damaged structure of polyamide layers as reported by others (Figure 6c). It was reported that CNTs in the polyamide can increase the chemical stability to the chlorine.[60] We believe that the interaction between the carboxylic acid group of the functionalized CNTs and the amide groups in the polymer matrix makes the membranes increase the chemical resistance to the chlorine.

We could have compared the membrane performances of PA-CNT4 membranes with those of commercial polyamide RO membranes. Although it is well-known that the active polyamide layers of the commercial polyamide RO membranes contain a various of additives to improve the membrane properties.[61,62] We also found that when the active top layers of PA-CNT4 membranes were coated with dilute aqueous solution of poly(vinyl alcohol), salt rejection value increased up to 99% without much decrease of the water flux, if any. Therefore, other additives included into the polyamide active layer of PA-CNT4 membranes possibly can increase the membrane performances; then they can be compared with those of the commercial RO membrane containing additives. However, the main object of this manuscript is to investigate the effect of CNTs in the active polyamide layer on the membrane performance. Therefore, we intentionally prepared the PA membranes without CNTs and PA-CNT membranes containing CNTs from the exact same method and their membrane performance behavior was compared. Currently, we are preparing other types of PA-CNT membranes with various additives and also using CNTs modified with various methods. Membrane performance of such PA-CNT membranes will be reported in near future, and then we can compare the membrane performance of our membranes with other commercial RO membranes.

CONCLUSION

We have demonstrated a strategy to prepare RO membranes having high water flux and high salt rejection behavior from the interfacial polymerization of trimesoyl chloride (TMC) solutions and *m*-phenylenediamine (MPD) using functionalized CNTs. When the functionalized CNTs were prepared by the reactions of pristine CNTs with a sulfuric acid and nitric acid mixture for 4 h at 65 °C, maximum flux and salt rejection values were observed. When shorter reaction time and lower reaction temperature were used, the CNTs were not well-dispersed in the polyamide active layers, and when longer reaction time and higher reaction temperature were used, CNTs were cut down into very small pieces to form aggregated structures. The good dispersion of the functionalized CNTs in the polyamide layer was ascribed to the high interactive force between the polyamide matrix with CNT, which could be confirmed from various characterization techniques including Raman spectro-

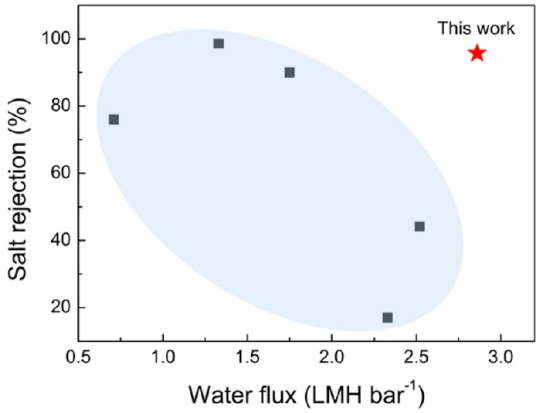

Figure 7. Comparison of the result in this work with other results by others for NaCl separation membranes containing CNTs (detailed information is in the Supporting Information, Table S1).

scopic mapping and interaction force measurements. The membranes containing the properly modified CNTs (PA-CNT4) demonstrates outstanding membrane performances, surpassing the recent upper bounds of polyamide membranes containing CNTs for NaCl separation system (Figure 7). The RO membrane containing the CNTs also showed improved durability and chemical resistance against NaCl solution compared with the RO membrane without any CNTs. Our results clearly show that properly functionalized CNTs can improve the membrane performance including membrane stability, possibly because of the unique properties of CNT such as hydrophobic surface property and high compression resistance.

■ ASSOCIATED CONTENT

Supporting Information

Additional tables and figures: Functionalization procedure of AFM tip to polyamide repeating unit (Figure S1), XPS spectra of CNTs in Table 1 of main manuscript (Figure S2), O/C ratios of CNTs modified in various conditions (Figure S3), SEM micrographs of top and bottom surfaces of PA and PA-CNT membranes (Figures S4 and S5), TEM images for membrane cross-section (Figure S6), typical force−extension curves recorded with a polyamide-modified tip against CNTs and their interaction force histograms (Figures S7 and S8), SEM micrographs of PA-CNT4 membrane (Figure S9), contact angles of PA, PA-CNT1, and PA-CNT4 membranes measured by captive bubble method (Figure S10), pure water flux of PA and PA-CNT4 membranes with time (Figure S11), mechanical properties of PA and PA-CNT4 membrane tested by UTM (Figure S12), membrane separation performances in current works in membranes with CNT (Table S1), water flux and salt rejection values of PA-CNT4 membranes from different monomer and CNT concentrations (Table S2), and surface compositions of polyamide-modified silicon wafer and polyamide membrane (Table S3). This material is available free of charge via the Internet at http://pubs.acs.org.

■ AUTHOR INFORMATION

Corresponding Author

*E-mail: jongchan@snu.ac.kr. Phone: +82 2 880 7070. Fax: +82 2 888 1604.

Notes

The authors declare no competing financial interest.

■ ACKNOWLEDGMENTS

This research was supported by the National Research Foundation of Korea Grant funded by the Korean Government (NRF-2010-C1AAA01-0029061) and the K-water Research & Business Project (K_RBP-1).

■ REFERENCES

(1) Potts, D. E; Ahlert, R. C.; Wang, S. S. *Desalination* **1981**, *36*, 235−264.
(2) Kang, G. D; Cao, Y. M. *Water Res.* **2012**, *46*, 584−600.
(3) Li, D.; Wang, H. T. *J. Mater. Chem.* **2010**, *20*, 4551−4556.
(4) Greenlee, L. F.; Lawler, D. F.; Freeman, B. D.; Marrot, B.; Moulin, P. *Water Res.* **2009**, *43*, 2317−2348.
(5) Lee, K. P.; Arnot, T. C.; Mattia, D. *J. Membr. Sci.* **2011**, *370*, 1−22.
(6) Pendergast, M. M.; Hoek, E. M. V. *Energy Environ. Sci.* **2011**, *4*, 1946−1971.
(7) Cha, B. J.; Yang, J. M. *Macromol. Res.* **2006**, *14*, 596−602.
(8) Alkhudhiri, A.; Darwish, N.; Hilal, N. *Desalination* **2012**, *287*, 2−18.
(9) Wu, C. R.; Jia, Y.; Chen, H. Y; Wang, X.; Gao, Q. J.; Lu, X. L. *Desalin. Water Treat.* **2011**, *34*, 2−5.
(10) Nghiem, L. D.; Hildinger, F.; Hai, F. I.; Cath, T. *Desalin. Water Treat.* **2011**, *32*, 234−241.
(11) Kosutic, K.; Kunst, B. *Desalination* **2002**, *150*, 113−120.
(12) Colquhoun, H. M.; Chappell, D.; Lewis, A. L.; Lewis, D. F.; Finlan, G. T; Williams, P. J. *J. Mater. Chem.* **2010**, *20*, 4629−4634.
(13) Park, S. Y; Kim, S. T.; Chun, J. H.; Chun, B. H.; Kim, S. H. *Desalin. Water Treat.* **2012**, *43*, 221−229.
(14) Park, H. B; Freeman, B. D; Zhang, Z. B.; Sankir, M.; McGrath, J. E. *Angew. Chem., Int. Ed.* **2008**, *47*, 6019−6024.
(15) Li, Q. L.; Elimelech, M. *Environ. Sci. Technol.* **2004**, *38*, 4683−4693.
(16) Qiu, S.; Wu, L. G.; Zhang, L.; Chen, H. L.; Gao, C. J. *J. Appl. Polym. Sci.* **2009**, *112*, 2066−2072.
(17) Paul, D. R. *Science* **2012**, *335*, 413−414.
(18) Fathizadeh, M.; Aroujalian, A.; Raisi, A. *J. Membr. Sci.* **2011**, *375*, 88−95.
(19) Li, J. F.; Xu, Z. L.; Yang, H.; Yu, L. Y.; Liu, M. *Appl. Surf. Sci.* **2009**, *255*, 4725−4732.
(20) Hu, M.; Mi, B. X. *Environ. Sci. Technol.* **2013**, *47*, 3715−3723.
(21) Li, J. B.; Zhu, Z. W.; Zheng, M. S. *J. Appl. Polym. Sci.* **2007**, *103*, 3623−3629.
(22) Lu, L. Y.; Sun, H. L.; Peng, F. B.; Jiang, Z. Y. *J. Membr. Sci.* **2006**, *281*, 245−252.
(23) Huang, H.; Qu, X. Y.; Dong, H.; Zhang, L.; Chen, H. L. *RSC Adv.* **2013**, *3*, 8203−8207.
(24) Uragami, T.; Okazaki, K.; Matsugi, H.; Miyata, T. *Macromolecules* **2002**, *35*, 9156−9163.
(25) Shi, Z.; Zhang, W. B.; Zhang, F.; Liu, X.; Wang, D.; Jin, J.; Jiang, L. *Adv. Mater.* **2013**, *25*, 2422−2427.
(26) Karan, S.; Samitsu, S.; Peng, X. S.; Kurashima, K.; Ichinose, I. *Science* **2012**, *335*, 444−447.
(27) Dror-Ehre, A.; Adin, A.; Mamane, H. *Desalin. Water Treat.* **2012**, *48*, 130−137.
(28) Hinds, B. J.; Chopra, N.; Rantell, T.; Andrews, R.; Gavalas, V.; Bachas, L. G. *Science* **2004**, *303*, 62−65.
(29) Choi, J. H.; Jegal, J.; Kim, W. N. *J. Membr. Sci.* **2006**, *284*, 406−415.
(30) Holt, J. K.; Park, H. G.; Wang, Y. M.; Stadermann, M.; Artyukhin, A. B.; Grigoropoulos, C. P.; Noy, A.; Bakajin, O. *Science* **2006**, *312*, 1034−1037.
(31) Thomas, J. A.; McGaughey, A. J. H. *Nano Lett.* **2008**, *8*, 2788−2793.
(32) Hummer, G.; Rasaiah, J. C.; Noworyta, J. P. *Nature* **2001**, *414*, 188−190.
(33) Gethard, K.; Sae-Khow, O.; Mitra, S. *ACS Appl. Mater. Interfaces* **2011**, *3*, 110−114.
(34) Kang, S.; Herzberg, M.; Rodrigues, D. F.; Elimelech, M. *Langmuir* **2008**, *24*, 6409−6413.
(35) Tiraferri, A.; Vecitis, C. D.; Elimelech, M. *ACS Appl. Mater. Interfaces* **2011**, *3*, 2869−2877.
(36) Vatanpour, V.; Madaeni, S. S.; Moradian, R.; Zinadini, S.; Astinchap, B. *J. Membr. Sci.* **2011**, *375*, 284−294.
(37) Chakraborty, A. K.; Plyhm, T.; Barbezat, M.; Necola, A.; Terrasi, G. P. *J. Nanopart Res.* **2011**, *13*, 6493−6506.
(38) Sahoo, N. G.; Cheng, H. K. F.; Bao, H. Q.; Li, L.; Chan, S. H.; Zhao, J. H. *Macromol. Res.* **2011**, *19*, 660−667.
(39) Peng, F. B.; Hu, C. L.; Jiang, Z. Y. *J. Membr. Sci.* **2007**, *297*, 236−242.
(40) Shawky, H. A.; Chae, S. R.; Lin, S. H.; Wiesner, M. R. *Desalination* **2011**, *272*, 46−50.
(41) Yu, M.; Funke, H. H.; Falconer, J. L.; Noble, R. D. *Nano Lett.* **2009**, *9*, 225−229.
(42) Du, F.; Qu, L. T.; Xia, Z. H.; Feng, L. F.; Dai, L. M. *Langmuir* **2011**, *27*, 8437−8443.

(43) Chan, W. F.; Chen, H. Y.; Surapathi, A.; Taylor, M. G.; Hao, X. H.; Marand, E.; Johnson, J. K. *ACS Nano* **2013**, *7*, 5308−5319.
(44) Li, J. S.; Zhang, Y. L.; To, S.; You, L. D.; Sun, Y. *ACS Nano* **2011**, *5*, 6661−6668.
(45) Zhi, L. J.; Fang, Y.; Kang, F. Y. *New Carbon Mater.* **2011**, *26*, 5−8.
(46) Zhai, D. Y.; Liu, B. R.; Shi, Y.; Pan, L. J.; Wang, Y. Q.; Li, W. B.; Zhang, R.; Yu, G. H. *ACS Nano* **2013**, *7*, 3540−3546.
(47) Wilson, J. T.; Keller, S.; Manganiello, M. J.; Cheng, C.; Lee, C. C.; Opara, C.; Convertine, A.; Stayton, P. S. *ACS Nano* **2013**, *7*, 3912−3925.
(48) Qiu, S.; Wu, L. G.; Pan, X. J.; Zhang, L.; Chen, H. L.; Gao, C. J. *J. Membr. Sci.* **2009**, *342*, 165−172.
(49) Rahmat, M.; Das, K.; Hubert, P. *ACS Appl. Mater. Interfaces* **2011**, *3*, 3425−3431.
(50) Chang, T. E.; Jensen, L. R.; Kisliuk, A.; Pipes, R. B.; Pyrz, R.; Sokolov, A. P. *Polymer* **2005**, *46*, 439−444.
(51) Bassil, A.; Puech, P.; Landa, G.; Bacsa, W.; Barrau, S.; Demont, P.; Lacabanne, C.; Perez, E.; Bacsa, R.; Flahaut, E.; Peigney, A.; Laurent, C. *J. Appl. Phys.* **2005**, *97*, 34303−34304.
(52) Poggi, M. A.; Lillehei, P. T.; Bottomley, L. A. *Chem. Mater.* **2005**, *17*, 4289−4295.
(53) Klare, J. E.; Murray, I. P.; Goldberger, J.; Stupp, S. I. *Chem. Commun.* **2009**, 3705−3707.
(54) Bahr, J. L.; Tour, J. M. *J. Mater. Chem.* **2002**, *12*, 1952−1958.
(55) Flavin, K.; Kopf, I.; Del Canto, E.; Navio, C.; Bittencourt, C.; Giordani, S. *J. Mater. Chem.* **2011**, *21*, 17881−17887.
(56) Kong, C. L.; Kanezashi, M.; Yamomoto, T.; Shintani, T.; Tsuru, T. *J. Membr. Sci.* **2010**, *362*, 76−80.
(57) Ghosh, A. K.; Jeong, B. H.; Huang, X. F.; Hoek, E. M. V. *J. Membr. Sci.* **2008**, *311*, 34−45.
(58) Jeong, B. H.; Hoek, E. M. V.; Yan, Y. S.; Subramani, A.; Huang, X. F.; Hurwitz, G.; Ghosh, A. K.; Jawor, A. *J. Membr. Sci.* **2007**, *294*, 1−7.
(59) Zou, H.; Jin, Y.; Yang, J.; Dai, H. J.; Yu, X. L.; Xu, J. *Sep. Purif. Technol.* **2010**, *72*, 256−262.
(60) Anantachaisilp, S.; Smith, S. M.; Treetong, A.; Pratontep, S.; Puttipipatkhachorn, S.; Ruktanonchai, U. R. *Nanotechnology* **2010**, *21*, 125102−125113.
(61) del Corro, E.; Izquierdo, J. G.; Gonzalez, J.; Taravillo, M.; Baonza, V. G. *J. Raman Spectrosc.* **2013**, *44*, 758−762.
(62) Kozielski, M.; Buchwald, T.; Szybowicz, M.; Blaszczak, Z.; Piotrowski, A.; Ciesielczyk, B. *J. Mater. Sci.: Mater. M.* **2011**, *22*, 1653−1661.
(63) Mendoza, A. J.; Hickner, M. A.; Morgan, J.; Rutter, K.; Legzdins, C. *Fuel Cells* **2011**, *11*, 248−254.
(64) Ingle, T.; Dervishi, E.; Biris, A. R.; Mustafa, T.; Buchanan, R. A.; Biris, A. S. *J. Appl. Toxicol.* **2013**, *33*, 1044−1052.
(65) Banerjee, S.; Hemraj-Benny, T.; Wong, S. S. *Adv. Mater.* **2005**, *17*, 17−29.
(66) Bokobza, L.; Zhang, J. *Express Polym. Lett.* **2012**, *6*, 601−608.
(67) Gao, Y.; Li, L. Y.; Tan, P. H.; Liu, L. Q.; Zhang, Z. *Chin. Sci. Bull.* **2010**, *55*, 3978−3988.
(68) do Nascimento, G. M.; Barros, W. P.; Kim, Y. A.; Muramatsu, H.; Hayashi, T.; Endo, M.; Pradie, N. A.; Fantini, C.; Pimenta, M. A.; Dresselhaus, M. S.; Stumpf, H. O. *J. Raman Spectrosc.* **2012**, *43*, 1951−1956.
(69) Barber, A. H.; Cohen, S. R.; Wagner, H. D. *Appl. Phys. Lett.* **2003**, *82*, 4140−4142.
(70) Kim, D. G.; Kang, H.; Han, S.; Lee, J. C. *J. Mater. Chem.* **2012**, *22*, 8654−8661.
(71) Hu, Z.; Li, J.; Tang, P. Y.; Li, D. L.; Song, Y. J.; Li, Y. W.; Zhao, L.; Li, C. Y.; Huang, Y. D. *J. Mater. Chem.* **2012**, *22*, 19863−19871.
(72) Celik, E.; Park, H.; Choi, H.; Choi, H. *Water Res.* **2011**, *45*, 274−282.
(73) Liu, M. H.; Wu, D. H.; Yu, S. C.; Gao, C. J. *J. Membr. Sci.* **2009**, *326*, 205−214.
(74) Glater, J.; Hong, S. K.; Elimelech, M. *Desalination* **1994**, *95*, 325−345.
(75) Junwoo, P.; Wansuk, C.; Kim, S. H.; Chun, B. H.; Joona, B.; Lee, K. B. *Desalin. Water Treat.* **2010**, *15*, 198−204.
(76) Zhao, L.; Chang, P. C. Y.; Ho, W. S. W. *Desalination* **2013**, *308*, 225−232.
(77) Lau, W. J.; Ismail, A. F.; Misdan, N.; Kassim, M. A. *Desalination* **2012**, *287*, 190−199.
(78) Zhao, H.; Qiu, S.; Wu, L.; Zhang, L.; Chen, H.; Gao, C. J. *J. Membr. Sci.* **2014**, *450*, 249−256.
(79) Roy, S.; Ntim, S. A.; Mitra, S.; Sirkar, K. K. *J. Membr. Sci.* **2011**, *375*, 81−87.
(80) Shen, J. N.; Yu, C. C.; Ruan, H. M.; Gao, C. J. *J. Membr. Sci.* **2013**, *442*, 18−26.
(81) Wu, H.; Tang, B.; We, P. *J. Membr. Sci.* **2013**, *428*, 425−433.
(82) Wu, H.; Tang, B.; We, P. *J. Membr. Sci.* **2010**, *362*, 374−383.
(83) Baek, Y.; Kang, J.; Theato, P.; Yoon, J. *Desalination* **2012**, *303*, 23−28.
(84) Corry, B. *J. Phys. Chem. B* **2008**, *112*, 1427−1434.
(85) Song, C.; Corry, B. *J. Phys. Chem. B* **2009**, *113*, 7642−7649.
(86) Amini, M.; Jahanshahi, M.; Rahimpour, A. *J. Membr. Sci.* **2013**, *435*, 233−241.